Astron. & Astrophys. 1, 54—61 (1969)

A Remnant of a Large-Scale Explosive Event in the Galactic Plane Around Longitude 60°

P. KATGERT
Sterrewacht Leiden

Received November 8, 1968

From observations of the 21-cm line of neutral hydrogen it appears that a peculiar object exists in the galactic plane around longitude 60°. The object is remarkable in that its radial velocity exceeds the maximum velocity corresponding to the adopted rotation curve by about 7 km/s. The internal velocity dispersion in the object is about 3.5 km/s (in one coordinate) and the mean surface density is 2.6×10^{20} H atoms/cm^2. The ring-like structure (diameter $\approx 4°$) suggests that the object originated from an explosive event.

Key words: 21 cm line, Galaxy — Supernovae remnants, Galaxy — explosive event.

1. Introduction

During a study of galactic rotation from observations of the 21-cm neutral hydrogen line Shane and Bieger-Smith (1966) noted a remarkable extension on the positive-velocity side of the line profile at $l = 63\overset{\circ}{.}0$, $b = 0\overset{\circ}{.}0$[1].

Their aim was to determine the galactic H I rotation curve and in the analysis of their profiles they therefore neglected this extension, describing it as probably being due to an isolated feature. Nothing could be said about the nature of the object which causes the extension because their observations were restricted to the galactic plane with an interval in longitude of one degree.

The extension of the profile is due to gas which moves with velocities that are larger than the velocity which at the subcentral point corresponds to the adopted rotation curve. For this reason it seemed worthwhile to study the feature in more detail.

Observations made around the position mentioned above show that the feature is present also at other positions, especially outside the galactic plane. It appears that the feature has a ring-like structure centred at $l = 61\overset{\circ}{.}5$, $b = -0\overset{\circ}{.}3$, while some filaments, which need not be physically connected with the ring, are seen at longitudes below 59°0.

2. The Observations and Their Reduction

The line profiles used in this study were obtained with the 25-metre Dwingeloo paraboloid, which at 1420 MHz has a halfpower beamwidth of $0\overset{\circ}{.}6$. The bandwidth of the intermediate-frequency stage of the receiver was chosen to be 8 kHz which gives a velocity resolution of about 1 km/s. The r.m.s. deviation of an individual point in the averaged profile with this bandwidth and a total integration time per half bandwidth of 60 s is 0.3 °K.

Fig. 1 shows the positions at which line profiles have been measured. Altogether 458 line profiles are used in the analysis. At 204 positions at least two independent profiles were averaged, while at 32 positions only one profile could be used. It is intended to publish the observed line profiles in a forthcoming issue of Astronomy and Astrophysics Supplement Series. The total observing time involved was about 100 hours.

The standard reduction of the observations was done with an Electrologica X 1 electronic computer using a program which, apart from some minor changes, is identical to the one described by Raimond (1966). In the reduction of the profiles no correction has been made for the effects of side-lobe radiation. When observing in the galactic plane around longitude 60° the main contribution to side-lobe radiation comes from the galactic anticentre. As we do not expect from this direction any appreciable amount of radiation at the line frequencies we are interested in, the corrections are assumed to be very small. More serious errors are expected to result from the dependence of the instrumental zero-level upon elevation and feed temperature. These errors are estimated to be some tenths of a degree.

The averaged brightness temperatures were converted to optical depths using a kinetic gas temperature T of 135 °K which was taken to be independent of position. It is of course doubtful whether T may be assumed constant over the distances involved (presumably several tens of parsecs), but until data on the distribution of cloud

[1] The galactic coordinates used in the following are based on the new system.

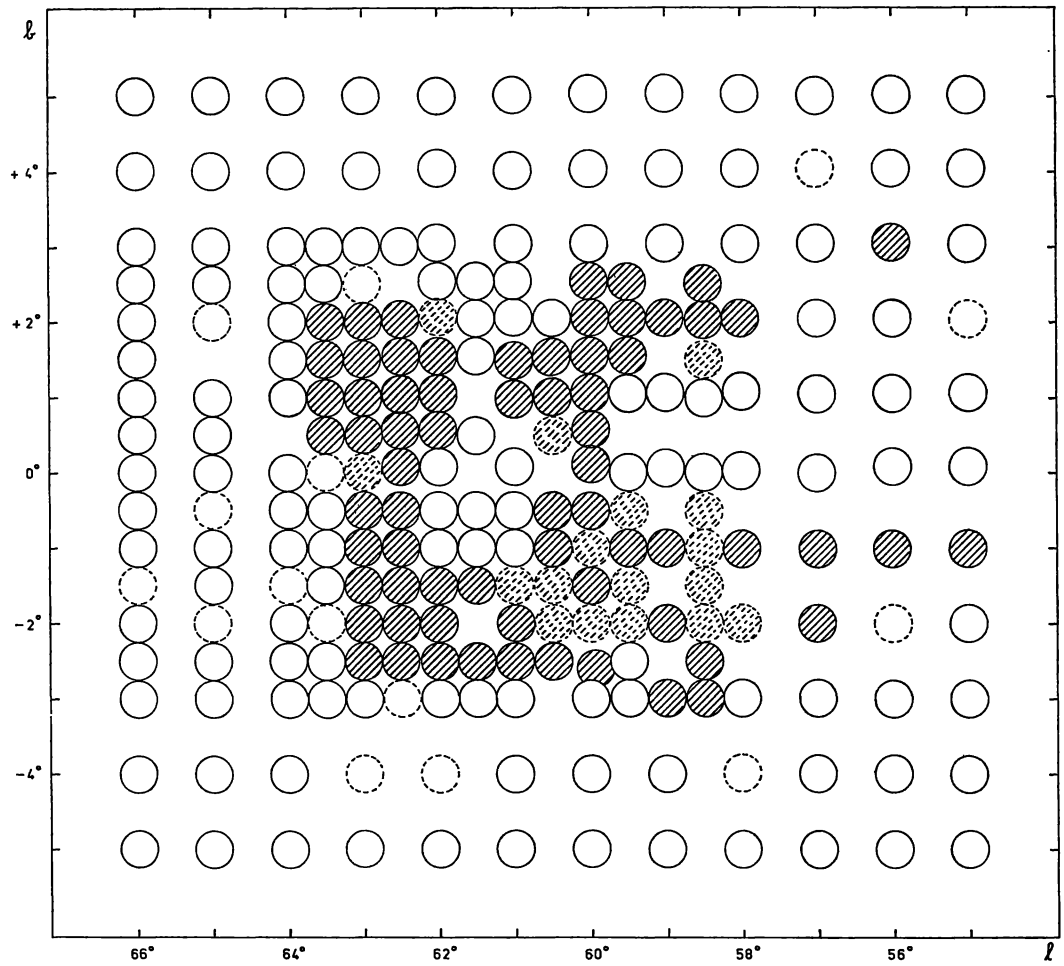

Fig. 1. The observed positions are indicated by circles with a diameter slightly less than the halfpower beamwidth at 21 cm of the Dwingeloo telescope. Positions where at least two line profiles were averaged are denoted by full-drawn circles, the others are indicated by dashed circles. At those positions where the circles have been hatched, gas with velocities larger than the adopted rotational velocity appeared to be present

temperatures become available one can do little better. The adopted value of 135 °K is rather high but the results are quite insensitive to the particular value of T employed.

3. Separation of the Radiation of the Object from the Galactic Background

At most positions where the object appeared to be present it is visible as a wing, starting from the flank of the last positive-velocity maximum in the profile and extending towards higher positive velocities. In only a few cases (e.g. $l = 63°$, $b = 0°$) does the object cause a distinct shoulder or a separate maximum.

In order to determine the properties of the object it obviously is necessary to have some knowledge of how the profile would look like if the object were not present. In our case such "no object" profiles were interpolated from positions where the object evidently is not present. The interpolation was done using contour maps of equal optical depth in the (V, l) plane for different latitudes b (the contour map at $b = -1.^{\circ}0$ is shown in Figure 2). Neglecting small-scale structure, the lines of equal optical depth are represented by smooth lines; for instance, in the contour map at $b = -1.^{\circ}0$, the structure around longitudes 58° and 63° is neglected.

An interpolation of this kind can e.g. be described by the general form of the contours of equal optical depth and the dependence of this form upon latitude, together with the distribution of optical depth with latitude (which is a function of velocity).

The interpolation on which the analysis is based has the following characteristics:

a) the contour maps are symmetric with respect to $b = 0°$;

b) the curvature of the contours increases with increasing latitude;

c) the distribution of optical depth with latitude has been represented by a gaussian, with a mean dispersion (for the velocity interval considered) of 3.3 degrees.

It is clear from Figure 3 that at some positions the interpolation does not give very good results. E.g. at $l = 58°.0, b = +2°.0$ and $l = 60°.5, b = -0°.5$ the interpolated profiles appear to be systematically higher than the observed ones at the low-velocity side. The opposite effect can be observed e.g. at $l = 59°.9$, $b = +1°.1$ where no clear maximum is visible, or at $l = 61°.5$, $b = -1°.5$ and $l = 62°.5$, $b = -2°.0$ where no

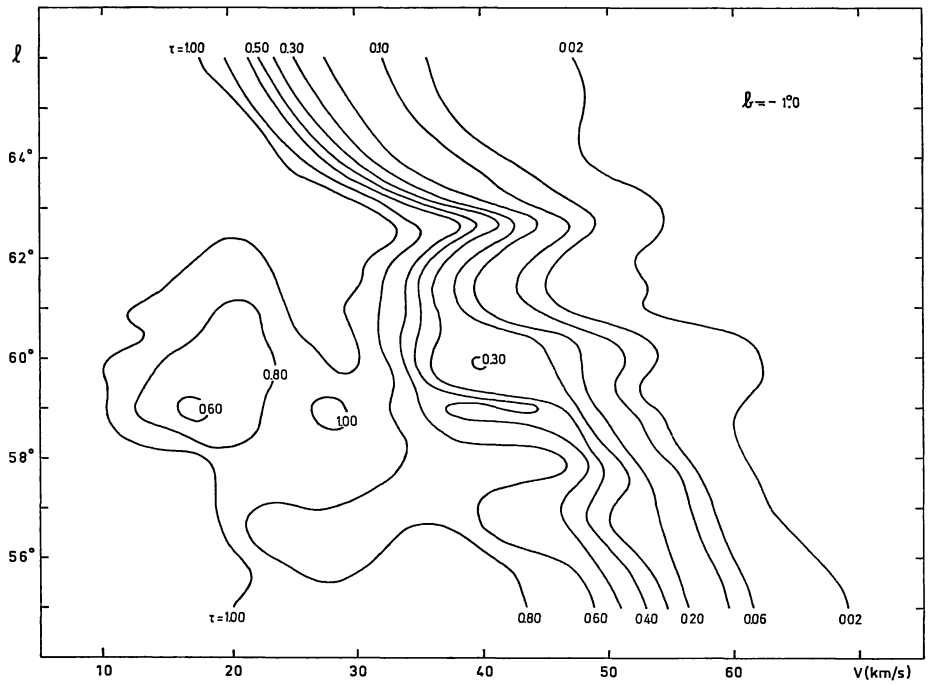

Fig. 2. Contour map of optical depth at $b = -1°.0$. Abscissae: radial velocities relative to l.s.r.; ordinates: longitudes. The object is clearly visible as it causes the extensions of the contours at $l = 58°$ and 63° respectively

This interpolation, though far from being ideal, was considered to give a sufficient representation of the observed contour maps, because at positions where the object obviously is not present, the differences between observed and computed profiles are more or less free from systematic effects.

4. Analysis of the $\Delta\tau$ Profiles

The interpolated profiles, computed for a velocity interval of 20 km/s, have been subtracted from the observed ones. Some of the resulting $\Delta\tau$ profiles ($\Delta\tau = \tau_{obs} - \tau_{comp}$) in which the object is visible are shown in Figure 3. It must be noted that to the right of the small vertical lines on the horizontal axes τ_{obs} is shown, in order to give an idea of the zero-line deviations.

maximum occurs at all. To what extent these defects of the interpolation influence the determination of the object's properties is discussed below.

For the 85 $\Delta\tau$ profiles which show the object the following quantities have been determined: the mean velocity V_0, the maximum optical depth τ_0, the surface density N_H and the dispersion in radial velocity σ.

a) In practice V_0 was taken to be the radial velocity of the maximum in the profile, because it was not always possible to determine the mean velocity because of incompleteness. If a maximum optical depth does not occur, or is hard to define (in about 20 per cent of the cases), V_0 is estimated on the basis of V_0 at neighbouring positions. Mean velocities estimated in this way are marked in Figure 6. When the maximum is clearly defined the uncertainty of

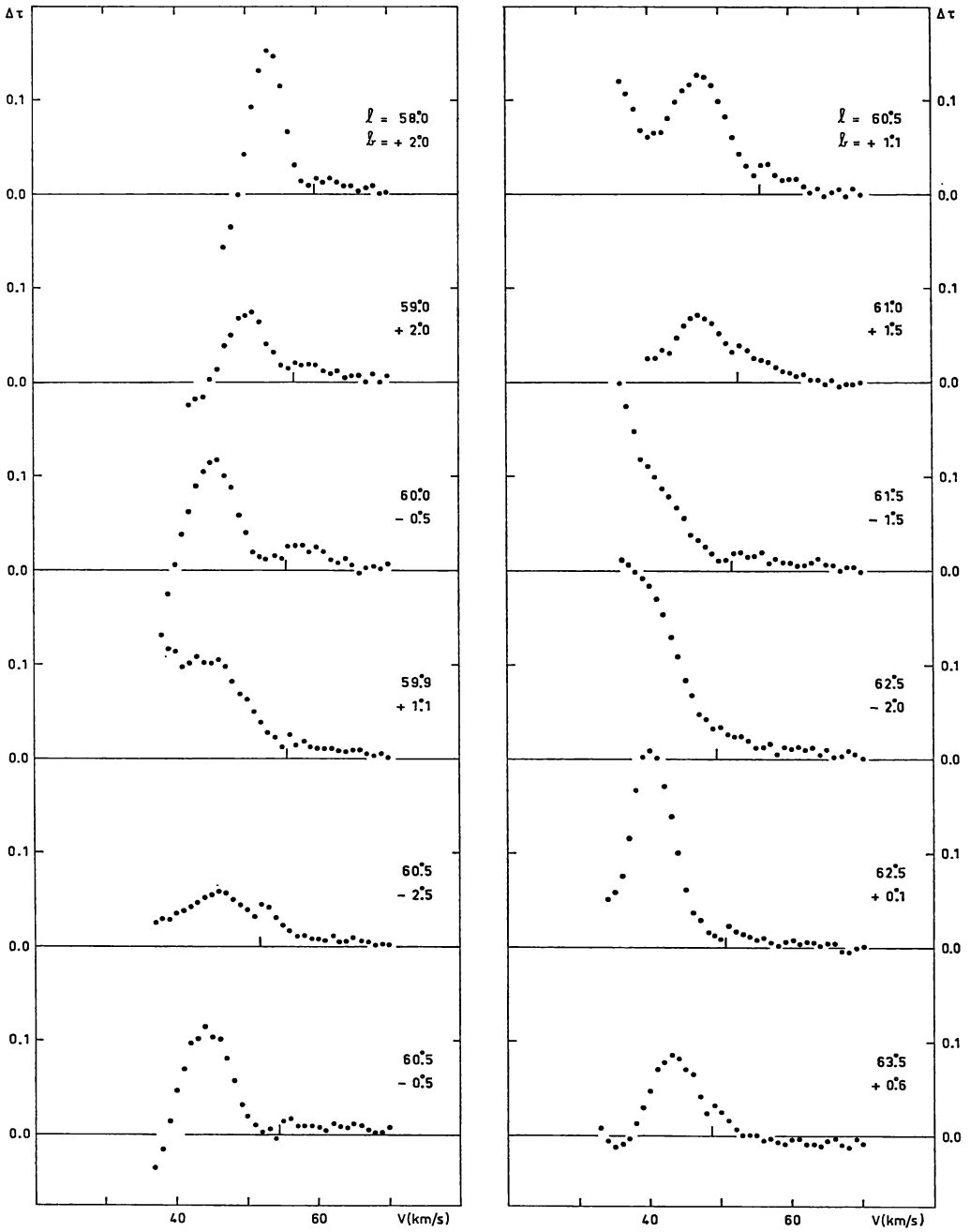

Fig. 3. Some $\Delta\tau$ profiles at positions where the object appeared to be present. The parts of the profiles to the right of the short vertical lines on the horizontal axes give the original optical depths τ_{obs}

V_0 is about 1 km/s. For the difficult profiles the uncertainty may be as large as 3 to 4 km/s.

b) The optical depth τ_0 can easily be determined for about 80 per cent of the cases, with an accuracy of 0.01 to 0.02. For these profiles the errors in τ_0 are caused mainly by the interpolation. If τ_0 cannot be measured directly (i.e. when V_0 is inferred from neighbouring values) an estimate is made for τ_0 which may have an error as large as 0.05.

c) The surface density is computed from $N_H = 1.83 \times 10^{18} T \int \tau(V)\, dV$ used in the form $N_H = 2.48 \times 10^{20} \Sigma\tau(V)\, \Delta V$ (with ΔV in km/s, N_H is in atoms/cm^2). Sometimes it appeared necessary to take two times $\Sigma\tau\,(V \geqq V_0)\, \Delta V$ instead of $\Sigma\tau(V)\, \Delta V$ because of incompleteness.

d) The velocity dispersion follows from $\sigma = V(\tau_0) - V(0.6\,\tau_0)$ (assuming a gaussian profile). The uncertainty in σ is about 1 km/s but may in some cases

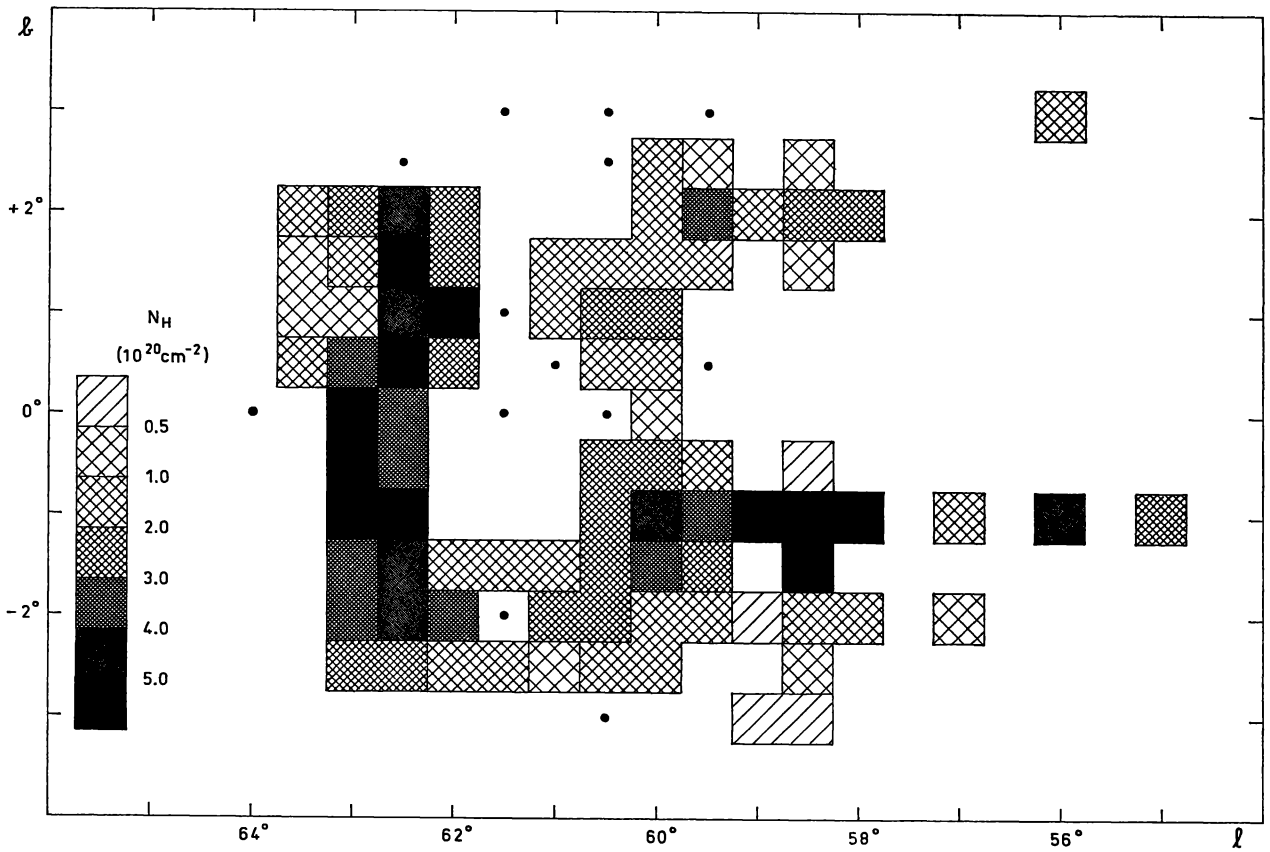

Fig. 4. Distribution of surface density over the object. Solid circles indicate positions in the region $59\overset{\circ}{.}5 \leqq l \leqq 64\overset{\circ}{.}0$, $-3\overset{\circ}{.}0 \leqq b \leqq +3\overset{\circ}{.}0$ which have not been observed. The positions where N_H has a large uncertainty, are identical to those in Fig. 5 where V_0 has been underlined

be larger. When $\Sigma\tau(V)\,\Delta V$ could well be determined we also computed the dispersion from $\sigma' = (\Sigma\tau(V)\Delta V)/((2\pi)^{1/2}\tau_0)$. The differences between σ and σ' were always smaller than the uncertainty in σ. For the badly defined profiles $\Sigma\tau(V)\,\Delta V$ was not only computed straightforward but also from $\Sigma\tau(V)\,\Delta V = \sigma\tau_0(2\pi)^{1/2}$ where τ_0 and σ are both rough estimates. The two values thus computed in general did not differ by more than 20 per cent. The mean value of σ is about 3.5 km/s.

Figure 4 shows the surface density distribution and Figure 5 the values of V_0. Positions inside the region $59\overset{\circ}{.}5 \leqq l \leqq 64\overset{\circ}{.}0 - 3\overset{\circ}{.}0 \leqq b \leqq +3\overset{\circ}{.}0$ which were not observed have been indicated by small circles in order to distinguish them from observed positions where the object has not been found.

Figures 4 and 5 suggest that the object may consist of two parts: 1) a ring-like component around $l = 61\overset{\circ}{.}5$, $b = 0\overset{\circ}{.}0$ with an angular diameter of about four degrees and 2) some filaments outside the galactic plane at longitudes $l \leqq 59°$. An argument in favor of such a separation is the jump in radial velocity around longitude 59°. In order to investigate this question in more detail the object was divided into two parts depending upon whether the radial velocity is larger or smaller than 48 km/s. Although the choice of this velocity is slightly arbitrary, the results are not influenced significantly if another velocity in the range 46—50 km/s is used. The dashed line in Figure 5 shows the corresponding division. The ring-like component has a centre of mass velocity of 42.3 km/s and a mean residual velocity of 2.8 km/s. For the filaments these numbers are, respectively, 51.5 and 1.8 km/s. It is difficult to understand a difference of 9 km/s in the centre of mass velocities of two parts of a single object, where the mean residual velocities in the various parts of the object are only of the order of 2.5 km/s.

The relative motion of the object (in the radial direction) with respect to its surroundings can only be determined if the distance from the sun is known. As a first approximation, however, the relative motion with respect to the gas at the subcentral points may be computed. The upper part of Figure 6

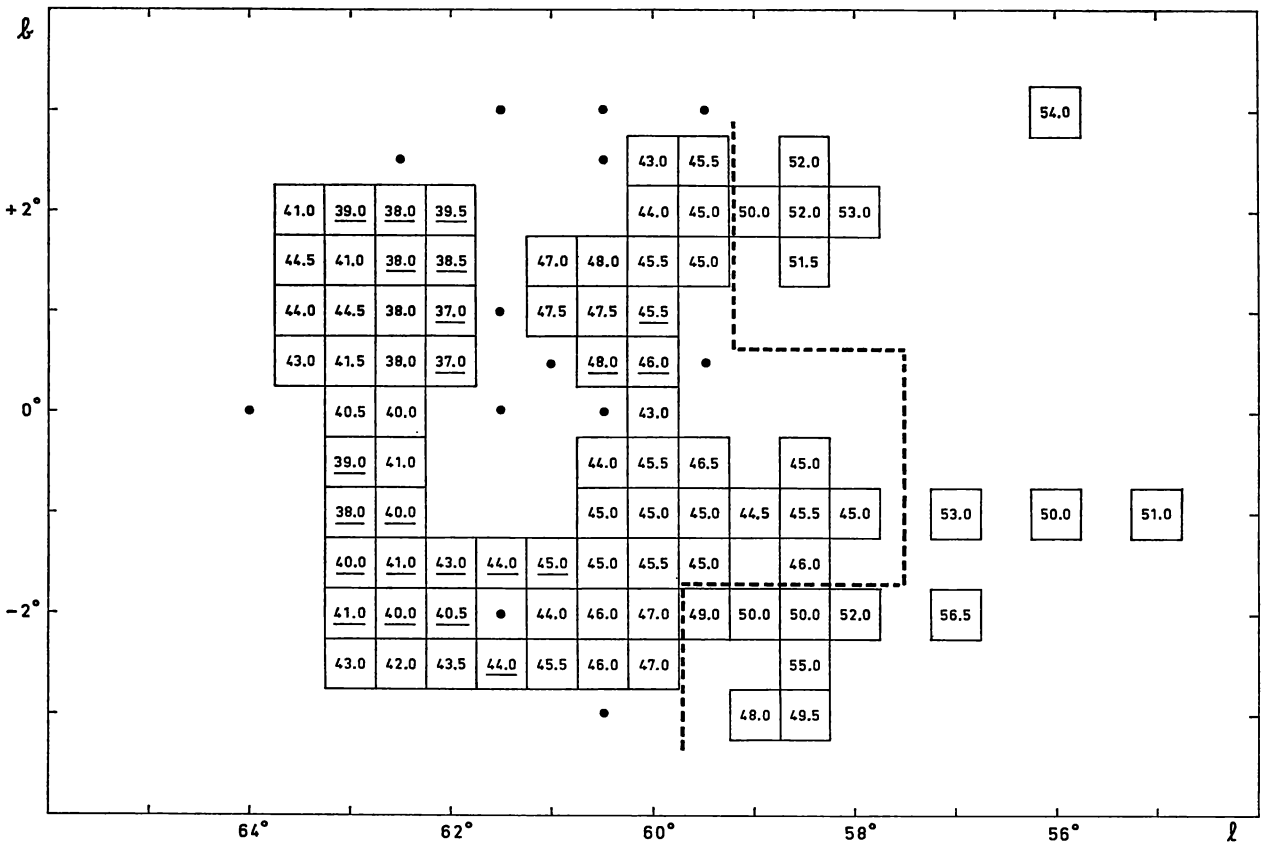

Fig. 5. The radial velocity V_0 of the object. The values of V_0 which could not be determined directly and consequently have a larger uncertainty are underlined. The dashed line shows the division between the supposed components depending upon whether V_0 is smaller or larger than 48 km/s. Solid circles have the same meaning as in Fig. 5

shows $V_0(l)$ (i.e. $V_0(l, b)$ averaged over latitude), together with $V_x(l)$, a measure of the terminal velocity of the profile. The values of $V_x(l)$ are taken from Shane and Bieger-Smith (1966) (column 7 of their table 1), who computed V_x on the assumption of an irregular rotation curve (their model VII). The lower part of Figure 6 shows $\Delta V(l) = V_0(l) - V_x(l)$; for the longitudes 58° and 59°, it gives the two components combined as well as separately. In order to find the relative motion with respect to the object's actual surroundings, a positive term of unknown magnitude which depends upon the distance of the object and probably varies with longitude must be added to $\Delta V(l)$.

The two maxima in the ΔV curve, for $l = 57°$ and 61° respectively, indicate that also from this point of view the object may be considered to consist of two parts. It is true that V_x used in Figure 6 has been calculated and thus differs from the observed V_x. Using the observed values for V_x (Shane and Bieger-Smith, column 3 of table 1) results in a slight change in ΔV. The maxima (in particular the one at $l = 61°$) become less pronounced but remain visible.

The mass of the object is $1.3 \times 10^4 r^2 M_\odot$ (r being the distance from the sun in kpc). This is a lower limit to the total neutral hydrogen mass, as the grid of observations did not completely cover the area, particularly in the region of the filaments. However, as the latter contribute only about ten per cent, the incomplete coverage can only slightly affect the total mass.

5. Interpretation

The, admittedly rather weak, resemblance with a ring suggests that the object might be regarded as a shell. From Figure 6 it can be seen that if this hypothetical shell expands at all its velocity of expansion cannot be much larger than the random velocities of the gas. The shell which presumably has acquired its present form by some sort of expansion, must therefore have been decelerated almost completely. As a consequence the centre of mass velocity of the shell must have become practically equal to

the average velocity of the medium in which the deceleration took place. This consequence of the above interpretation is in contrast with the observations; it was just its velocity relative to the interstellar medium that made the object conspicuous. It is therefore very unlikely that we observe a complete, totally decelerated, shell.

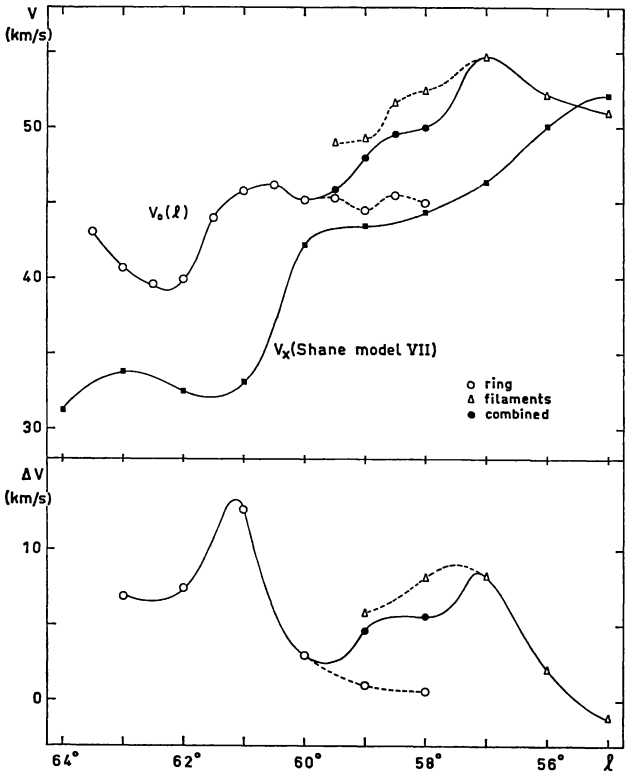

Fig. 6. The relative motion of the object with respect to the gas at the subcentral points. In the upper part of the figure $V_0(l)$ and $V_x(l)$ are shown, while the lower part gives $\Delta V = V_0 - V_x$. Between longitudes 57° and 60° velocities are given for the entire object as well as for the ring and the filaments separately

It remains quite possible, however, that what we observe is *part* of an expanding shell that has not been completely decelerated, and of which we observe only the rear half which moves away from us; the approaching gas is lost in the ordinary low-velocity gas. This model requires the expansion of the shell together with the motion of its centre of mass to yield a maximum radial velocity that is at least 7 km/s larger than the local rotational velocity. Many specific models can of course be made which fulfill this condition but it should be remembered that also the following restriction must be observed. The translational momentum of the shell with respect to the surrounding medium will be smaller than the momentum of the decelerating shell, i.e. the expansion velocity will have to be larger than the peculiar velocity of the shell's centre of mass.

There is one objection against the above interpretation that has to be mentioned. If the interpretation in terms of an expanding shell is correct one would expect to see a more or less circular feature in which the surface density decreases towards the centre. The largest velocities occuring at the centre would certainly be expected present although the integrated density will be lower than at the edges. The complete lack of gas at the centre of the object is therefore somewhat unexpected. It might be due to anisotropy of the shell or to irregularities in the decelerating medium. Although this absence of gas cannot be explained in detail, it would not seem to be a decisive objection against the proposed interpretation.

The distance of the object, which of course cannot be determined directly may be estimated by means of the following, very simple model. Assume M_0 solar masses to have been ejected isotropically in a medium with uniform density ϱ_0. The swept up matter forms a shell with total mass

$$M_{\rm tot}(R) = M_0 + \frac{4}{3}\pi\,\varrho_0\,R^3 = \frac{1}{q}M_{\rm obs}$$

(R is the radius of the shell at a particular moment, q is the fraction of the total mass that is observed). Substituting $M_{\rm obs} = 1.2 \times 10^4\, r^2\, \mathrm{M}_\odot$ (the shell only) and $R = 0.035\, r$ we obtain, neglecting M_0,

$$\varrho_0 = \frac{3}{qr}\ (\varrho_0 \text{ in H atoms/cm}^3,\ r \text{ in Kpc}).$$

The value of q will be in the range $0.5 \leqq q \leqq 0.7$ so that $\varrho_0\, r = 4$ to 6. Because *mean* hydrogen densities larger than 2 atoms/cm³ occur very rarely it appears from the foregoing that r probably is larger than 2 kpc. An interpretation in terms of a nearby (r about 100 pc) expanding shell seems to be completely impossible.

Making use of the same simple model, we may estimate the initially ejected amount of matter as well as the age of the object. Assuming $2 \leqq r \leqq 8$ kpc (a distance interval symmetric around the subcentral point) and estimating the initial expansion velocity as $V_0 = 7500$ km/s we find, if momentum is conserved and with a present velocity in the range 10 to 20 km/s: $100 < M_0 < 4000\, M_\odot$. The initial mass, required if the object is the result of an explosive event appears to be much larger than the masses ejected during supernova explosions. The large amount of matter may have been furnished by a *series* of supernova explosions, taking place in a

time interval that is short compared with the age of the object which with the same model would be 1 to 7 million years. This age is sufficiently large to make a series of, say 1000 supernova explosions possible in e.g. ten per cent of the total time available. The large amount of energy (10^{53} to 10^{54} ergs) released during the early phases of the expansion need not necessarily have been furnished by a series of explosions. It may also have come from what sometimes has been referred to as a super supernova explosion.

It is of interest to investigate whether the object is possibly related to a stellar association. In this connection it is appropriate to recall the existence of the two neutral hydrogen clouds observed eight degrees South of the h and χ Persei cluster. Blaauw (1962) suggested that these clouds may be related to the cluster, as the radial velocity of the cluster is just in between those of the clouds. The clouds may have gained their momentum relative to the cluster both from thermal expansion or supernova explosions.

The only known association close to the investigated feature is the Vulpecula I association around $l = 60°3$, $b = +0°1$. The distance of this association has been discussed by several authors, all on the basis of spectroscopic distance moduli of OB stars. Morgan *et. al.* (1953) find from six stars a distance of 1800 pc. Kopylov (1958), using ten stars, finds 2300 pc. The radial velocity of the association is according to Mohr and Mayer (1957) +18.8 km/s. A determination by Trumpler gives $V = +20$ km/s. In the following a distance of 2 kpc and a radial velocity of +20 km/s is assumed. If there is a relation between the object and the Vulpecula I association, the expansion velocity of the shell is at least 10 km/s (half the velocity of the receding part relative to the association). From this point of view it is, consequently, quite possible that such a relation exists. A distance of 2 kpc for our object would however imply a mean interstellar gas density of more than 2 atoms/cm^3. For this reason we think that the feature is not related to the association, but probably is located near the subcentral point, i.e. at a distance of about 5 kpc. In that case the neutral hydrogen mass of the object is $5 \times 10^5\ M_\odot$.

Acknowledgements. It is a pleasure to thank W. W. Shane who planned the first observations leading to this investigation and who gave much helpful advice during the course of this work. I would also like to thank both him and Professor J. H. Oort for their valuable criticism during the preparation of this paper.

References

Blaauw, A. 1962, Interstellar Matter in Galaxies, ed. L. Woltjer (Benjamin, New York) 63.
Kopylov, I. M. 1958, Soviet Astr. **2**, 359.
Mohr, J. M. and Mayer, P. 1957, Bull. Astr. Inst. Czechoslovakia, **8**, 142.
Morgan, W. W., Whitford, A. E. and Code, A. D. 1953, Ap. J. **118**, 318.
Raimond, E. 1966, Bull. Astr. Inst. Netherlands Suppl., **1**, 33.
Shane, W. W. and Bieger-Smith, G. P. 1966, Bull. Astr. Inst. Netherlands, **18**, 263.

P. Katgert
Sterrewacht Leiden
Leiden
The Netherlands